JOURNAL OF MATERIALS SCIENCE 33 (1998) 2447–2455

Self-sustaining oxidation of liquid aluminium and its alloys containing magnesium and silicon

E. C. PARTINGTON
Department of Industrial Engineering, University of Hong Kong, Pokfulam Rd, Hong Kong

P. GRIEVESON
Private Consultant, Surbiton, Surrey, UK

B. TERRY
Cunningham Miller and Terry Consulting, Chessington, KT92AX, UK

An experimental investigation has been conducted into factors affecting the self-sustaining air oxidation of liquid aluminium and its alloys containing magnesium and silicon. Thermogravimetry and optical microscopy, scanning electron microscopy, and X-ray diffraction analysis have been performed to characterize the progress of oxidation and the nature of the products produced. On the basis of the results obtained, a comprehensive model is proposed capable of explaining the observed capability of producing an alumina composite material by a self-sustaining oxidation mechanism. It is proposed that aluminium/alumina transport occurs by means of the formation of gas-phase aluminium-bearing species which are then encapsulated by a liquid MgO–SiO_2–Al_2O_3 slag phase. Subsequent precipitation of alumina from the slag phase provides the means by which alumina is continuously distributed throughout a growing alumina composite material.

1. Introduction

In 1985, Lanxide [1] revealed a patent for the production of a novel alumina/aluminium composite material. The patent describes how, under certain controlled conditions, some alloys of aluminium can be induced to undergo catastrophic oxidation in a controlled manner. The product of the process is a dense Al_2O_3 matrix infiltrated with the aluminium alloy. The aluminium alloy is claimed to fill a system of pores developed in the Al_2O_3 product of oxidation (the crust).

In order continuously to form the crust-like layer of Al_2O_3 composite material, certain conditions are required. Silicon and magnesium solutes in quantities varying between 1% and 10% by weight must be present in the aluminium alloy. The alloy must then be heated in air or oxygen to temperatures within an upper bound of 1400 °C and a lower bound of 1100 °C. Under such circumstances during a period measured in hours, the aluminium oxidizes to form the Al_2O_3 crust in a self-propagating reaction which only terminates when the aluminium melt is totally converted to alumina or when the temperature is allowed to move out of the operational limits.

To date there appears to have been no comprehensive mechanism put forward for this observed behaviour. In particular, questions arise as to:

(i) how does the aluminium react swiftly and continuously to form alumina when the formation of alumina would be expected to passivate the reaction?

(ii) what are the roles of silicon and magnesium in the process?

(iii) what factors determine the upper and lower temperature limits of the process?

(iv) how does the alumina become evenly distributed over the growing surface of the crust when it appears that aluminium is delivered to the surface by a pore system covering only a small fraction of the surface?

In the absence of added solutes, the formation of a solid alumina product surface layer is known to passivate the oxidation of liquid aluminium [2]. In the presence of dissolved magnesium catastrophic breakaway oxidation of aluminium–magnesium alloys has been observed in numerous works [3–8]. All works appear to be in close agreement concerning the events occurring and with their interpretation of the phenomena involved in the catastrophic oxidation. These can be summarized as follows. At temperatures above the melting point of the alloy, an amorphous film of MgO appears on the surface. Crystalline MgO and then spinel $MgAl_2O_4$ form, creating fragmented clusters infiltrated with aluminium metal. Oxidation and growth of the spinel occur at hot spots on the surface leading to rapid weight gain. Once the magnesium is exhausted, a substantial decrease in the rate of weight gain occurs.

Fig. 1 summarizes the observed behaviour. Clearly these types of phenomena are likely to occur during oxidation under the conditions of the Lanxide process.

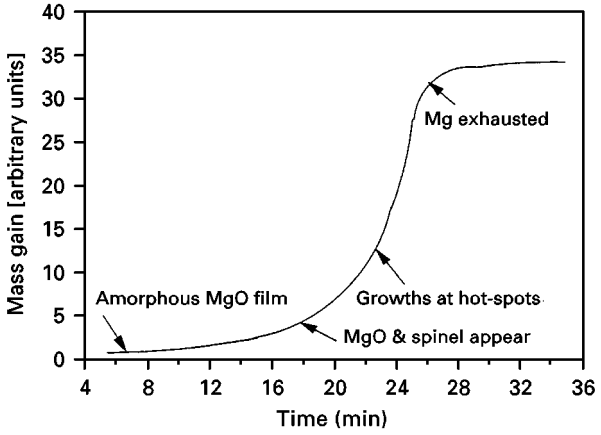

Figure 1 Typical oxidation behaviour of Al–Mg liquid alloys.

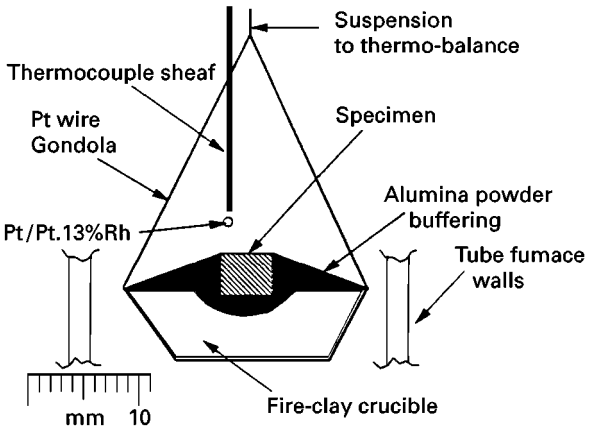

Figure 2 The experimental arrangement for the thermogravimetric experiments.

However, most of the phenomena detailed earlier remain unexplained.

Previous works have suggested that the presence of magnesium controls the basic oxidation process whilst silicon accelerates growth. Guillard *et al.* [9] have published equilibrium thermodynamic calculations of potential reactions in the Al/Al_2O_3 system in the presence of small quantities of magnesium and silicon. The amount of oxygen present is shown to be critical in determining whether aluminium oxide or nitride is formed.

The authors were also able to demonstrate that an Al/Al_2O_3 composite material could be successfully produced by the oxidation of pure aluminium with surface additions of 3 wt % each of magnesium, MgO and silicon.

The purpose of the present study was to conduct an experimental investigation of the oxidation of aluminium alloys under Lanxide patent conditions, with the aim of developing a comprehensive model for the observed behaviour. In addition, the Lanxide patent is reliant upon the use of aluminium alloys as described earlier. The present study further investigated the possibility of generating the required alloying additions by the *in situ* aliminothermic reduction of added oxides of magnesium and silicon. Thus it is envisaged that it may be possible to produce similar products to those of the Lanxide process by the oxidation of pure aluminium top dusted with silica and magnesia powder. This latter route is referred to in this study as the powder route, whereas the route as specified in the original Lanxide patent is referred to as the alloy route.

2. Experimental procedure

2.1. Aluminium alloy route

In this series of experiments, specimens containing various combinations of aluminium, silicon and magnesium were thermally cycled under a flow of air at temperatures in the range of 1100–1400 °C. Rates of reaction at a series of process temperatures were measured employing a thermogravimetric apparatus. Larger specimens were treated in a muffle furnace and the products of the oxidation process were examined by metallography and X-ray diffraction in order to assess the effects of temperature and alloy content upon the process.

2.2. Powder route

The conditions of the above alloy route experiments were replicated using superpure aluminium specimens top dusted with various mixtures of silica and magnesia. The powders were spread in an even layer 2 mm thick over the top of the surface.

2.3. Materials

Various alloys of aluminium–silicon–magnesium were made up from superpure aluminium, Al–8% Mg and Al–12.5% Si, provided by Alcan International.

For the thermogravimetric experiments, these were first cast into multiple 6 mm diameter holes drilled through a 30 mm thick steel block and were then sawn into 6 mm long cylindrical specimens.

Further casts were made on to a thick alumina disc to produce specimens for the muffle furnace experiments. These were approximately 80 mm diameter and 10 mm thick.

2.4. Thermogravimetric experiments

Fig. 2 shows the arrangement employed. The cylindrical specimens were embedded in fine alumina powder in a fireclay crucible of 25 mm diameter so that only the top surface was directly exposed to the atmosphere.

A platinum wire gondola was fashioned to hold the crucible and then to suspend it from a Stanton Redcroft thermogravimetric apparatus. The specimen thermocouple was suspended at a height of 3 mm above the specimen's top surface. The arrangement was lowered into a 35 mm diameter silica glass tube located in an electrically heated tube furnace. A flow rate of air of 200 °C min^{-1} was employed throughout the course of the experiment. The experiment consisted of heating the specimen at a rate of 250 °C h^{-1} to a predetermined temperature (normally 1250 °C) and then holding at that temperature until no further

weight gain was detected. In the case of the alloy route experiments, an alloy composite of Al–5% Si–5% Mg was employed, unless otherwise stated.

2.5. Muffle furnace experiments

The disc-shaped specimens were weighed and placed on a thick alumina disc and put into a muffle furnace. The temperature was raised at the rate of 250 °C h^{-1} until the desired temperature was reached. Dwell times at this temperature were selected to yield specimens at various stages in the formation of the crust. Temperatures were monitored by means of a Pt/Pt13%Rh thermocouple shielded by an alumina sheath. Spot checks of the temperature at the specimen surface were made by sighting a total radiation optical pyrometer through a shuttered hole prepared in the furnace roof. After each run the specimen was weighed and prepared for optical microscopy and X-ray analysis.

3. Results

3.1. Alloy route thermogravimetric experiments

Table I details the results of the experiments conducted using thermogravimetry and the alloy route. Fig. 3 shows a typical result obtained from the thermogravimetric experiments. Two significant weight gain events occurred. The first reaction occurred at around 950 °C and was attributed primarily to the oxidation of magnesium. A second more sustained reaction occurred at 1150–1250 °C corresponding to the continuous formation of alumina.

The first reaction paths for two alloys having Si : Mg ratios of 1 : 1 and 1.5 : 1, respectively, are plotted in Fig. 4. Each shows a sharp initiation point followed by an exponential rise for the major part of the weight gain and finally a terminal period during which the rate falls off smoothly during a glass formation stage.

The second reaction (or aluminium-ignition reaction) occurred after an incubation period of an hour and while the temperature of the furnace was rising through 1150 °C.

Subsequent runs were prepared employing a dwell time of 30 min at 1000 °C followed by a rapid raising of temperature to 1250 °C to trigger the second reaction deliberately. This second reaction occurred in two stages, the first stage comprising an exponential rise in weight over 25 min as shown in Figs 5 and 6. The second stage comprised a linear increase in weight which continued until the aluminium was exhausted.

3.2. Alloy route muffle furnace experiments

Table II details the results of the experiments conducted using the muffle furnace. The specimens, which were doped with both silicon and magnesium, became coated with a crusty skin of dark grey oxide at around 900–1000 °C. This was subsequently found to consist of spinel.

TABLE I Experimental programme: thermogravimetric series (alloy route)

Alloy Constitution	Spinel Forms	Alumina Forms	Temp. [°C]	Time [min]	Mass gain rate [mg/sec/cm^2]
Aluminium	NR	NR	NR	NR	NR
Al/12.5% Si	NR	NR	NR	NR	NR
Al/5% Mg	Yes	NR	860	NA	NR
Al/8% Mg	Yes	NR	770	NA	NR
Al/5% Mg/	Yes		890	NA	NR
5% Si		Yes	1240	73	0.33
Al/6% Si/	Yes		950	NA	NR
4% Mg		Yes	1223	65	0.53
Al 50%/Fe	NR		1400	60	NR
50%		Slight			

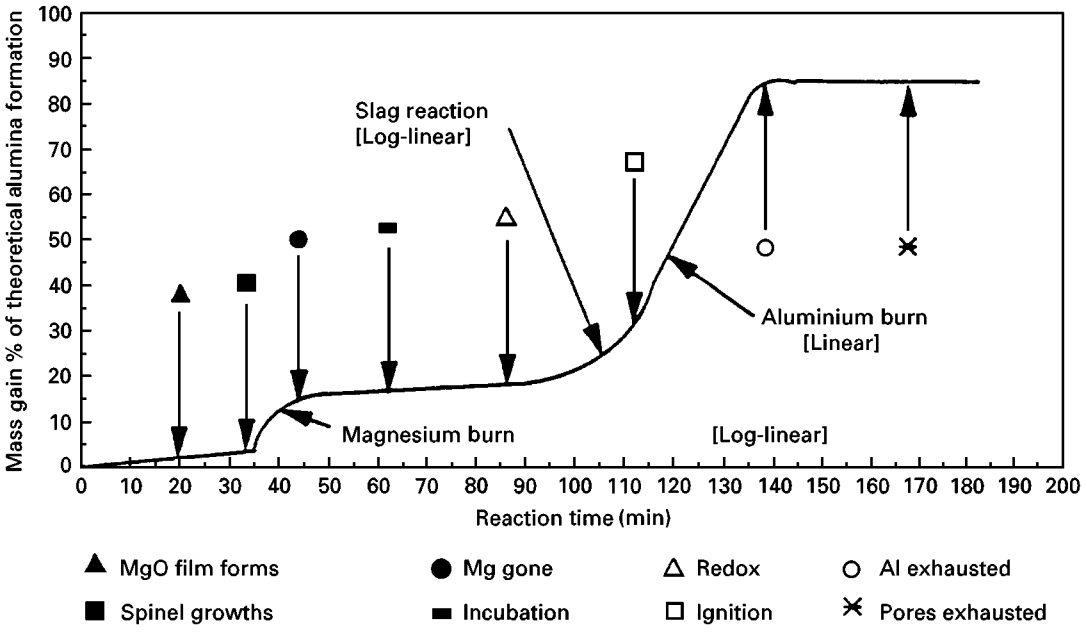

Figure 3 The typical course of the thermogravimetric experiment.

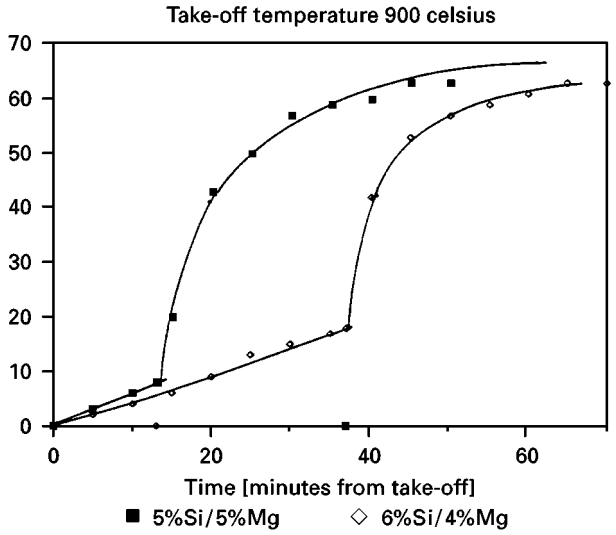

Figure 4 Magnesium oxidation and spinel formation during the oxidation of Al–Mg–Si alloys.

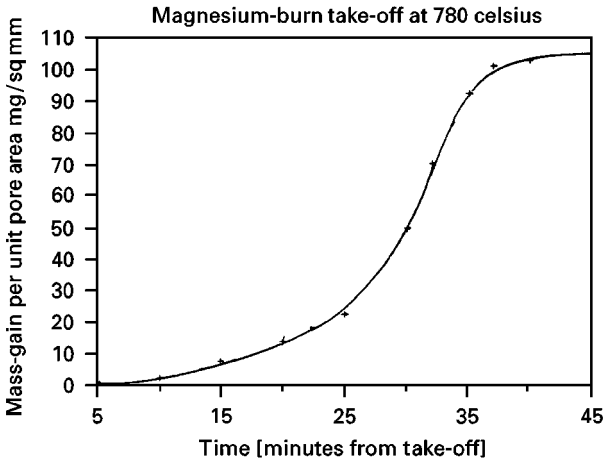

Figure 5 Initiation of aluminium oxidation in the reaction of Al–Mg–Si alloys.

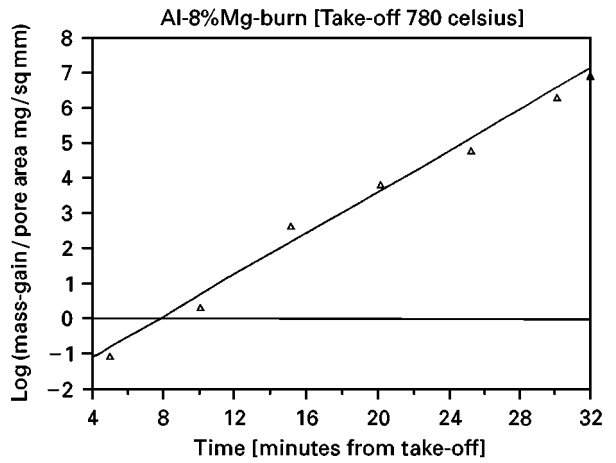

Figure 6 Initiation of aluminium oxidation in the reaction of Al–Mg–Si.

Specimens withdrawn from the furnace after times during which temperatures exceeded 1100 °C (that is to say after the second reaction had occurred) were coated with a crust of grey alumina, the thickness of which was directly related to the time. In general, a typical rate of growth in thickness was about $3\,mm\,h^{-1}$. These results confirm and provide support for the observations made and the conclusions drawn from the thermogravimetric experiments.

TABLE II Experimental programme: muffle furnace series (alloy route)

Alloy Constitution	Spinel Forms [R1]	Alumina Forms [R2]	Temp [°C] [R1/R2]	Time [R1–R2] [min]
Aluminium	NR	NR	NR	NR
Al/12.5% Si	NR	NR	NR	NR
Al/5% Mg	Yes	NR	856	NA
Al/8% Mg	Yes	NR	780	NA
Al/5% Mg	Yes		900	NA
+ 5% Si		Yes	1230	80
Al/6% Si +	Yes		950	NA
4% Mg		Yes	1223	67
Al/Fe50%	NR	Slight	1400	60

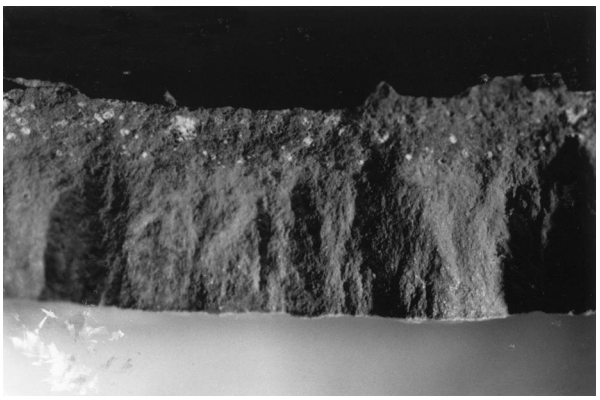

Figure 7 Cermet crust alloys formed by oxidation of Al–Mg–Si alloy.

Specimens which were allowed to go to completion until the aluminium was completely exhausted were found to contain a cavernous void conforming to the original shape of the specimen (Fig. 7). Microscopic examinations of the crust revealed a grey-coloured matrix infiltrated by a fine network of pores. The majority of the pores were fine, about 5 μm in diameter, and were aluminium filled. In addition there were some pores varying in size from 30–90 μm which were often empty in those specimens reacted to completion.

The top surface of the crust was found to be coated intimately with a thin 500 μm layer of a transparent glass. This was found to consist of a solidified alumina–silica–magnesia slag phase.

3.3. Powder route muffle furnace experiments

Table III details the results of experiments conducted in the muffle furnace employing the powder route. The results obtained indicated that an excellent alumina crust product could be obtained in the presence of MgO and SiO_2 conditions. If anything, this product was superior to that obtained by the alloy route

TABLE III Experimental programme: muffle furnace series (powder route)

Specimen Top Powders	Spinel Forms	Alumina Forms	Temp [°C]	Time [min]
Aluminium	NR	NR	NA	NA
Al/MgO	Yes	NR	780	NA
Al/Silica	NR	NR	NR	NA
Al/MgO	Yes		900	55
Silica		Yes	1200	
/Vanadium	NR	Yes	650	NA
PbO		[sponge]		
/Hematite	NR	NR	NA	NA
/Calcium	NR	NR	NA	NA
Fluoride				
/Sodium	Yes	[sponge]	851	NA
Carbonate	[calcine]	Yes	900	
/Potassium	Yes	[sponge]	891	NA
Carbonate	[calcine]	Yes	891	

TABLE IV Experimental series: thermogravimetric series (powder route)

Specimen /powder	Spinel Forms	Alumina Forms	Temp [°C]	Time [min]	Mass Gain Rate [mg/sec/cm^2]
Al/MgO	Yes	NR	860	NR	NA
Al/Silica	NR	NR	NR	NR	NA
Al/MgO	Yes		770	45	0.43
Silica		Yes			
Crucible	NR	Yes	1140	75	0.0145
Scrapings					
/Hematite	NR	Slight	1223	NA	0.0008
/Calcium	NR	Slight	1250	NA	0.0004
Fluoride					

consisting of a finer microstructure with fewer open pores or voids. The separate addition of either MgO and SiO_2 failed to produce satisfactory product.

3.4. Powder route thermogravimetric experiments

Table IV details the results of experiments conducted using thermogravimetry and the powder route. The results are similar to those obtained in the alloy route. Spinel formation commenced at 860 °C (comparable to the oxidation of Al–5% Mg) in the case of oxidation of Al/MgO and at 770 °C in the case of oxidation of Al/MgO/SiO_2. The latter figure is significantly lower than that previously observed for the oxidation of the Al–Mg–Si alloys studied. The rate of oxidation observed in the Al/MgO/SiO_2 system studied (0.43 mg s^{-1} cm^{-2}) was comparable to those previously observed for the oxidation of Al–Mg–Si alloys (0.33–0.53 mg s^{-1} cm^{-2}).

3.5. Oxidation of alumina alloys with restricted oxygen access

In the experiments reported to date, oxygen access was afforded both from the top and the sides of the specimen. In the case of the thermogravimetric experiments this arose as the porous alumina bed in which the specimen was located, as shown in Fig. 2, afforded access of oxygen to the sides of the specimen.

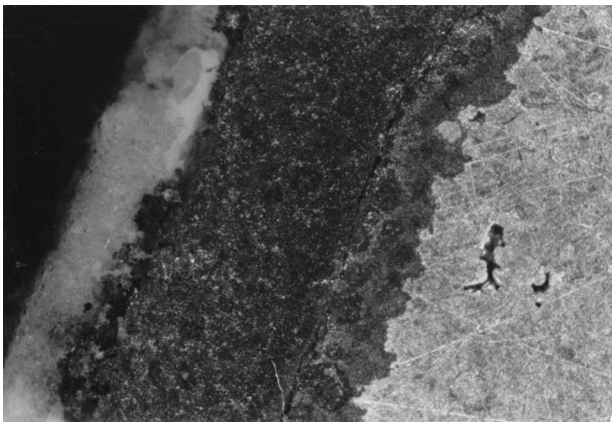

Figure 8 The layered crust formed during oxidation on the restricted oxygen access.

A single experiment was conducted in which oxygen access was totally restricted to the top surface. A cylindrical crystallized alumina crucible 3 cm diameter and 5 cm deep was filled to a depth of 3 cm by a molten Al–5%Mg–5%Si alloy. After solidification of the alloy, the crucible was placed in the muffle furnace and taken through a thermal cycle of 250 °C h^{-1} heating to a temperature of 1250 °C, 10 h dwell at 1250 °C and air cooling outside the furnace.

After cooling, the crucible contents were found to comprise a metal ingot capped by a multi-layered crust, about 3 mm thick, as shown in Fig. 8. These layers were identified by X-ray diffraction analysis to be alumina, magnesia and spinel ($MgAl_2O_4$) closest to the metal ingot surface. Scanning electron microscopy (SEM) analysis revealed that the spinel phase was infiltrated by aluminium through a pore network. This latter observation provides strong evidence of the excellent wetting of the spinel phase by the previously liquid aluminium.

It is pertinent that in this experiment the oxidation ceased before complete utilization of the available metal of the specimen. In normal circumstances, where oxygen access from the sides of the specimen as well as the top of the specimen was allowed, this did not occur. Thus it appears that the surface glass layer, being restricted only to the top surface of the specimen, reaches a sufficient thickness to cause a sufficient barrier to choke the oxidation process. This necessary thickness appears to be of the order of 3 mm.

4. Discussion

4.1. Mechanism of the Lanxide process

The Lanxide process is extremely complex and up to the present time no logical explanation has been presented in the literature for the observed behaviour. Several observations made in the present investigations have allowed a reaction scheme to be proposed.

Such a reaction scheme is now put forward and its validity explored in relation to observations made by

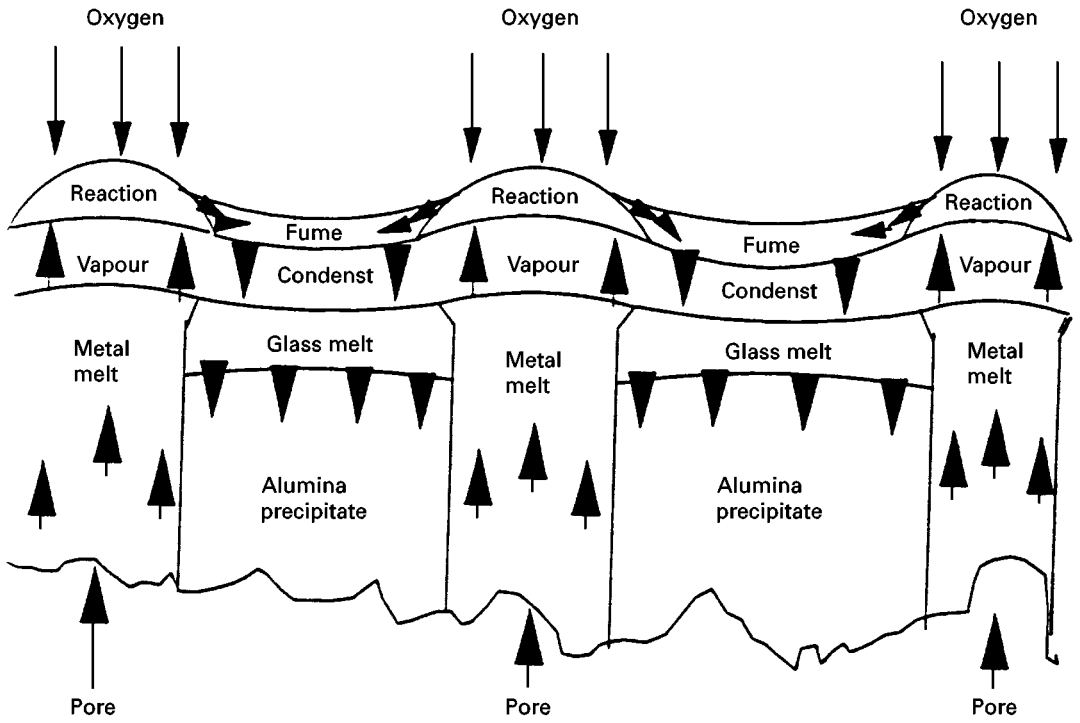

Figure 9 The reaction system for self-sustaining oxidation.

us and other workers and to relevant knowledge of high-temperature physical chemistry.

Fig. 9 depicts the reaction scheme we envisage being responsible for the steady-state self-sustaining oxidation of aluminium alloys to produce an alumina/aluminium composite material, as observed in the Lanxide process.

Notable features of this scheme are as follows:

(i) a porous skeleton of alumina has been formed,

(ii) a glass melt consisting of a slag of Al_2O_3, MgO and SiO_2 forms on top of the alumina skeleton. The slag constituents can be formed by oxidation of the alloy or by deliberate oxide addition;

(iii) liquid aluminium alloy rises through the pores of this skeleton by a wicking or capillary action. The surface of these pores remains accessible for access of oxygen to the oxidizing metal;

(iv) at the mouth of the pores, aluminium and/or aluminium sub-oxide vaporization occurs as a result of the formation of local hot spots;

(v) This vapour is oxidized to produce alumina, the exothermicity of the oxidation reactions aiding hot-spot formation;

(vi) the oxidized alumina forms as a condensed fume and is encapsulated by the glass melt;

(vii) temperature and concentration gradients within the glass melt permit dissolution of the condensed alumina at the top of the melt and precipitation of alumina on the existing alumina skeleton at the bottom of the melt as alumina saturation is reached;

(viii) A steady state is reached when the rate of heat generation from the oxidation reaction balances the heat losses from the reaction zones.

Each of the above features of our proposed reaction scheme are now critically examined.

4.2. Formation of alumina skeleton/preformation

The formation of an alumina skeleton requires that the formation of a coherent alumina film on the surface of the liquid aluminium is avoided. Thus, the initial oxide formed must be of such a structure as to allow penetration of liquid aluminium through the oxide film for further oxidations. The introduction of MgO into the system is considered to be critical in this respect, as it leads to the formation of a spinel with the alumina and so creates fragmentation of the oxide skin covering the melt.

In the absence of MgO additions, the introduction of MgO into the system is brought about by the oxidation of the magnesium content of the aluminium alloy. Under such conditions, there appears to be little doubt concerning the events which take place as reported by several independent workers [6, 8, 11].

The sequence of events commences with the formation of MgO at temperatures at or above 750 °C. The reduction in volume on oxidation is around 20% and hence the MgO forms a fragmented granular substrate constituting a seed bed for the subsequent growth of spinel ($MgAl_2O_4$) once aluminium oxidation commences. Further oxygen access to the aluminium is thus permitted.

In the powder route, control of the pore structure can be afforded by control of the particle size of MgO employed.

In contrast, in the alloy route, the fineness of the pores is likely to be related to the $MgO/MgAl_2O_4$ structure formed in the early stage of oxidation and hence by the rate of reaction in these early stages. As such, therefore, control of the pore size and structure is

likely to be more difficult in the alloy route compared to the powder route.

Terminal conditions occur when the reservoir of aluminium is exhausted.

4.3. Process temperature limits

The Lanxide patent limits the operational temperature regime as having an upper bound of approximately 1400 °C and a lower bound of around 1100 °C. The lower limit appears to coincide with the need for spinel formation and below this it would appear that insufficient spinel formation occurs to produce the necessary pore system and capillary transport. The upper bound is likely to be associated with the additional temperature rise giving rise to temperatures which result in excessive loss of aluminium from the system via the vapour phase.

4.4. Capillary transport

Once the porous substrate is formed, liquid aluminium rises up through pores by capillary attraction. The necessary low interfacial energy permitting this appears to result from and is aided by:

(i) the continuing presence of $MgO/MgAl_2O_4$ at the pore surface (at least in trace quantities) and throughout the pore system as it grows, and

(ii) the presence of dissolved magnesium in the liquid aluminium.

Previous work on the production of composite materials has, for example, shown that the presence of MgO strongly affects the interfacial tension permitting capillary rise of the aluminium metal.

The presence of the $MgO/MgAl_2O_4$ products has been confirmed in our experiments. In particular, experiments conducted with restricted oxygen access referred to earlier clearly demonstrated the production of these phases during the oxidation process. In particular, these experiments, as shown in Fig. 8, revealed the ready wetting of the spinel phase by the aluminium.

Ignition, reaction and alumina distribution are the core phenomena which are held to be responsible for the peculiar characteristics of the Lanxide process. The observed rates of reactions and the alumina distribution over the crust covering the pores lead us to conclude that gas-phase reactions are involved. For the layer of alumina formed by the oxidation reaction to remain porous and unblocked, it is necessary for a liquid phase to be generated out of the silica, magnesia and alumina formed by the oxidation reactions. It is also necessary that these oxidation reactions are sufficiently exothermic and occur sufficiently rapidly to raise the temperature enough to permit liquid slag formation.

4.5. Slag formation

The constituents of the liquid slag phase are the oxides of aluminium, magnesium and silicon. These may either form by oxidation of the alloy constituent by the atmosphere or in the case of MgO and SiO_2 may be added independently.

The following exothermic reactions may occur to provide sufficient heat for the generation of the liquid slag phase.

(i) Oxidation of silicon content of the alloy.

(ii) Oxidation of magnesium content of the alloy.

(iii) Oxidation of aluminium.

(iv) Exothermic formation of $MgAl_2O_4$ spinel from MgO and Al_2O_3.

(v) Exothermic reduction of added silica by the aluminium melt.

The ternary phase diagram of the Al_2O_3–MgO–SiO_2 system shown in Fig. 10 indicates a eutectic temperature of 1347 °C. Thus, the reaction detailed above must be sufficiently exothermic to raise the temperature to at least this value.

4.6. Alumina skeleton (crust) formation

The alumina skeleton growth is proposed to occur by precipitation from the ternary Al_2O_3–SiO_2–MgO at the cooler interface between the bottom of the slag layer and the existing alumina skeleton. The continued production of alumina by precipitation pins the slag composition in the alumina-saturated alumina valley of the Al_2O_3–SiO_2–MgO phase diagram.

Microscopic examination shows that the surface of the crust is not a flat featureless plain surface (Fig. 11), but rather consists of polyp-shaped growths in a sea of glass. The growths are about 100 μm across consisting of alumina radially permeated with aluminium-filled pores in cross-sections. Between the growths are voids which contain glass.

The finest structures (i.e. those with the smallest polyp growths) were obtained by way of the powder route. It is likely that the fineness of the pores can be controlled to an extent by the fineness of the powder employed in the powder route. The fineness of the pores will also ultimately determine the limiting thickness of the crust, as the finer the pore the greater will be the capillary forces acting.

4.7. Alumina transport

Our model indicates that the oxidation of alumina takes place locally at hot spots above the pores. Observations, however, show that alumina growth takes place more or less over the whole of the alumina skeleton crust and that this growth continues to take place without blocking the pores.

Our model accounts for this by proposing a cyclic process in which aluminium and alumina sub-oxide vaporization promote alumina transport from the pore mouths. Further oxidation in the gas phase leads to the formation of alumina. In some cases, this alumina formation has been found to occur as whiskers, as shown in Fig. 12. This observation of whisker formation is strong supporting evidence for the proposed role of gas-phase formation of alumina.

Once formed in the gas phase, the alumina falls on to the surface of the liquid slag where it is dissolved into, and consumed by, the slag phase.

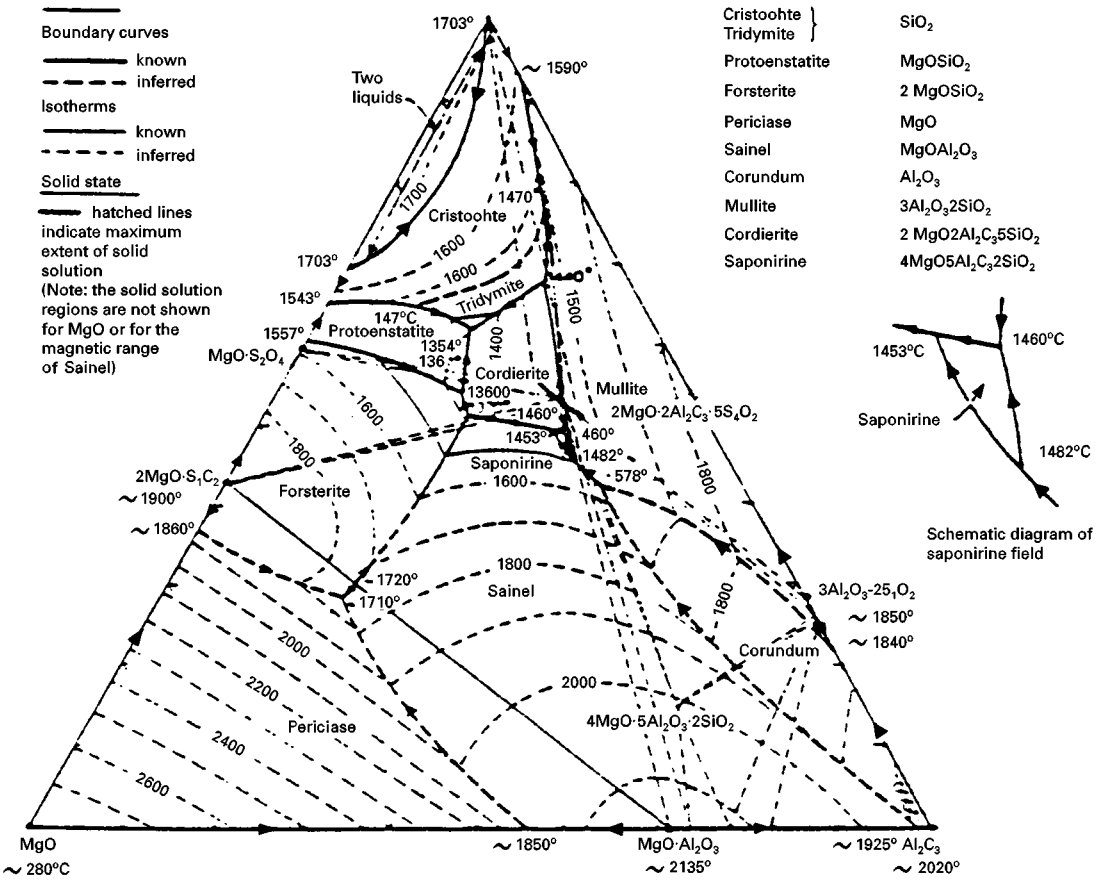

Figure 10 The ternary phase diagram of Al_2O_3–MgO–SiO_2.

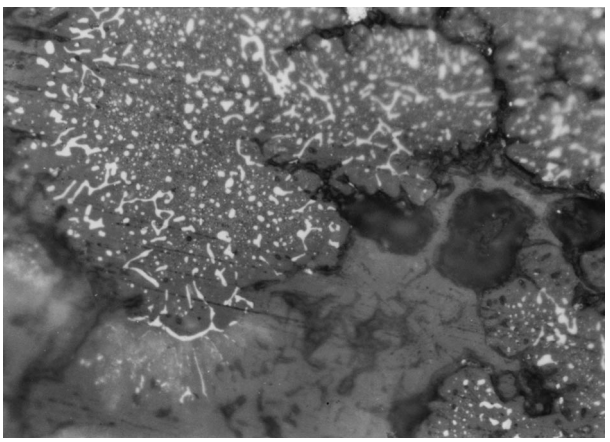

Figure 11 The nature of the crust surface during the course of oxidation.

Figure 12 Whisker formation at the top surface of the glass layer.

4.8. Summary of crust-formation mechanisms

The crust-formation mechanism relies upon a series of events. Catastrophic oxidation begins with the preferential formation of MgO. The volume of the oxide is some 20% less than the element and the MgO is therefore fragmented, allowing oxygen access to the virgin metal through fissures or pores.

Spinel forms from the MgO and alumina. This ensures the development of self-sustaining pores. The pore surface is probably a solid solution of spinel in alumina. This has a high surface energy and promotes the capillary ingress of the metal melt.

The steady-state stage of continuous formation of alumina at the top of the pores is preceded by an initiation stage where oxidation takes place in a reactive oxide slag. The slag is driven to and held at alumina saturation by oxidization of the rising metal. During this stage, alumina is continuously precipitated on the cooler surface of the crust, thus sustaining

the reaction. The system is not, however, in a state of thermal equilibrium. The rate at which exothermic heat is produced exceeds that at which it is transferred away, hence the temperature rises. Before thermal equilibrium can be achieved, the rising temperature alters the system conditions by creating metal vapours which undergo oxidation in the gas phase immediately above the melt.

Eventually, a limiting condition is encountered at which the oxygen diffusion rate in the gas phase is only just sufficient to oxidize the aluminium vapour at that temperature. Thus a dynamic equilibrium, or steady state, is achieved wherein the heat supplied by the reaction of the vapour with the limiting supply of diffusing oxygen is just sufficient to produce the requisite rate of vapour formation. However, transport of the sub-oxides of aluminium away from the oxygen-impoverished hot zones create further exothermic heat as they are transported over the glass layer where fresh oxygen supplies exist. This is the principal driving mechanism by which the alumina crust is formed.

A second approach to the process was investigated which involved the sprinkling of silica and magnesia powder on to the top surface of a pure alumina specimen prior to oxidation. This produced the same results as those obtained from oxidation of ternary Al–Mg–Si alloys. The use of surface oxide additions offers the advantage of cheaper starting materials and potentially greater control over the pore structure of the composite material products.

5. Conclusion

A comprehensive model has been proposed capable of explaining all observed features of the self-sustaining oxidation of alumina alloys. Notable features of the model include the role of the gas-phase transport of aluminium-bearing species and of a slag phase in permitting alumina distribution throughout the surface of the growing alumina product.

References

1. S. F. DIZIO, Eur. Pat. Appl. 155 831, 15/3/85 Lanxide Corporation Invention.
2. M. DROUZY and C. MAGORE, *Metall. Rev.* **131** (1960) 25.
3. R. DELAVAULT, *Bull Soc. Chim. Fr.* (1934) 319.
4. S. BALICKI, *Prace Inst. Hutn.* **10** (1958) 208.
5. S. BALICKI and J. LEITH, *ibid.* **11** (1959) 71.
6. W. VON THIELE, *Aluminium* **38** (1962) 707.
7. I. HAGINOYA and T. FUKUSAKO, *Trans. Jpn Inst. Metals* **24** (1983) 613.
8. C. N. COCHRAN, D. I. BELITSKUS and D. L. KINOSZ, *Metall. Trans.* **8** (1977).
9. G. WIGHTMAN and D. J. FRAY, *Metall. Trans. B* **12** (1993) 625.
10. F. J. A. GUILLARD, R. J. HARD, W. E. LEE and B. B. ARGENT, in "High Temperature Materials Chemistry", edited by B. C. H. Steele (The Institute of Materials, 1995) pp. 161–74.
11. M. SASABE and M. JIBIKII, *Can. Metall. Q.* **22** (1983) 29.
12. P. K. ROHTAGI, R. ASSTHAM and S. DAS, *Int. Metal Rev.* **31** (1986) 115.

Received 9 September 1996
and accepted 7 April 1997